

Embodiment of Low Operating Voltage in Positive Column AC-PDPs

Hyun Kim, Heung-Sik Tae, and Sung-Il Chien
 School of Electronic and Electrical Engineering,
 Kyungpook National University, Daegu 702-701, Korea
 Phone : +82-53-950-6563 , E-mail : hstae@ee.knu.ac.kr

Abstract

The positive column discharge characteristics in the long gap (440 μm) are investigated based on the voltage distribution among three electrodes. In particular, the effects of the amplitude and width of the short pulse applied to the address electrode on the positive column discharge characteristics are examined intensively. By proper controlling of the amplitude and width of the address short pulse, it is found that the positive column discharge in the long gap is well constructed. As a result, under the stable static voltage margin condition, the firing and sustaining voltages are as low as those of conventional short gap (60 μm) discharge ($V_f=220\text{V}$, $V_s=150\text{V}$) and the color purity is improved. Moreover, the luminous efficiency increases up to 60% in comparison with the conventional case.

1. Introduction

Many researches related to improving the luminous efficiency have been performed intensively for several years because the luminous efficiency in AC-PDP is still a big problem. However, the improvement of luminous efficiency under the restriction of short discharge gap (60~120 μm) gradually faces its limit. Thus, the demand on the new cell structure with the new driving scheme grows to take another way to improve the luminous efficiency in AC-PDP. It is well-known that the luminous efficiency of the discharge can be improved when the discharge is produced in the longer discharge gap with a positive column region. However, the firing and sustaining voltages increase in proportion to the length of the long discharge gap, even though the luminous efficiency increases with the length of the discharge gap. In this reason, the long gap discharge with a positive column is known to be not easily applicable to the current PDP with micro-discharge cells. Recently, regarding the positive column discharge, lowering firing and sustaining voltages and earning better luminous efficiency using negative sustaining voltage in AC-PDP is proposed as well as several modified ideas using auxiliary electrodes [1][2][3]. However, the firing voltage and the sustaining voltage is still higher than the conventional case. According to the positive column discharge characteristics reported by Weber [1], since the distance between two sustain electrodes is long, the initial discharge began to be produced between the sustain and address electrodes by applying the negative sustain voltage between two sustain electrodes [I : triggering discharge], then extending along the address electrode [II : discharge extending procedure]. Finally, the main discharge was produced between two sustain electrodes with long gap [III: long gap main discharge]. This type of discharge mechanism is quite adaptable to long gap three electrode micro cell structure. However the firing and sustaining voltages are still higher than that of the conventional short gap case.

In this paper, the long gap (440 μm) discharge characteristics are examined based on the control of the voltage distribution among

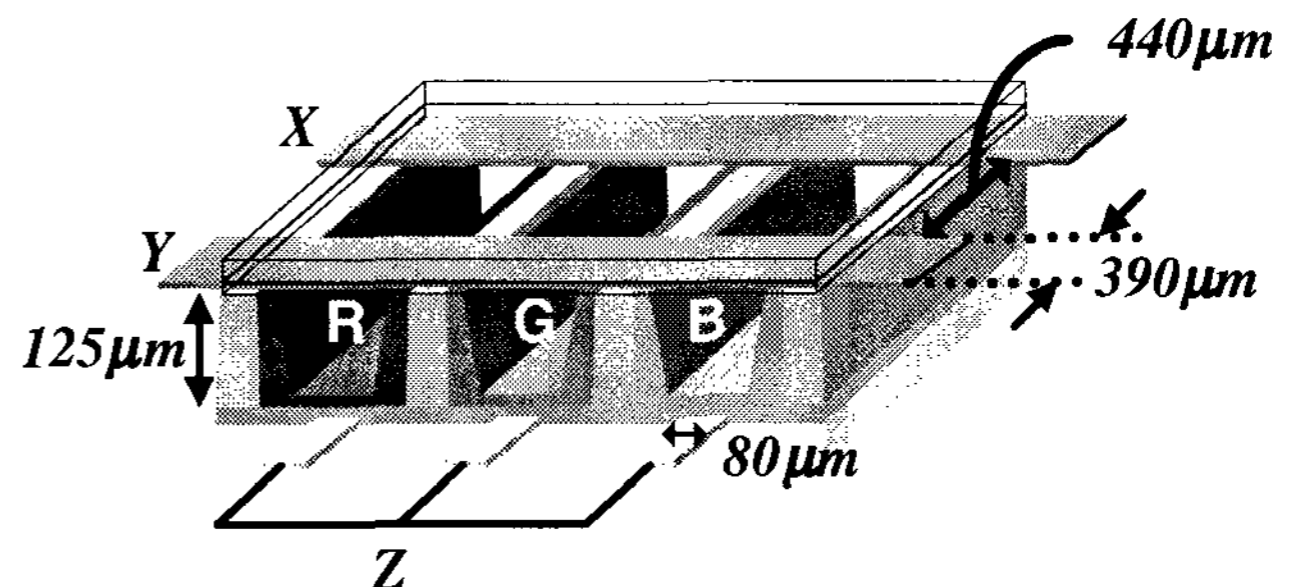


Fig 1. Cell structure for positive column discharge.

three electrodes for a positive column AC PDP. In particular, the effects of the amplitude and width of the address pulse applied to the address electrode, on the long gap discharge characteristics such as the firing voltage, sustain voltage, static voltage margin, luminous efficiency, and color purity, are investigated intensively.

2. Experiment

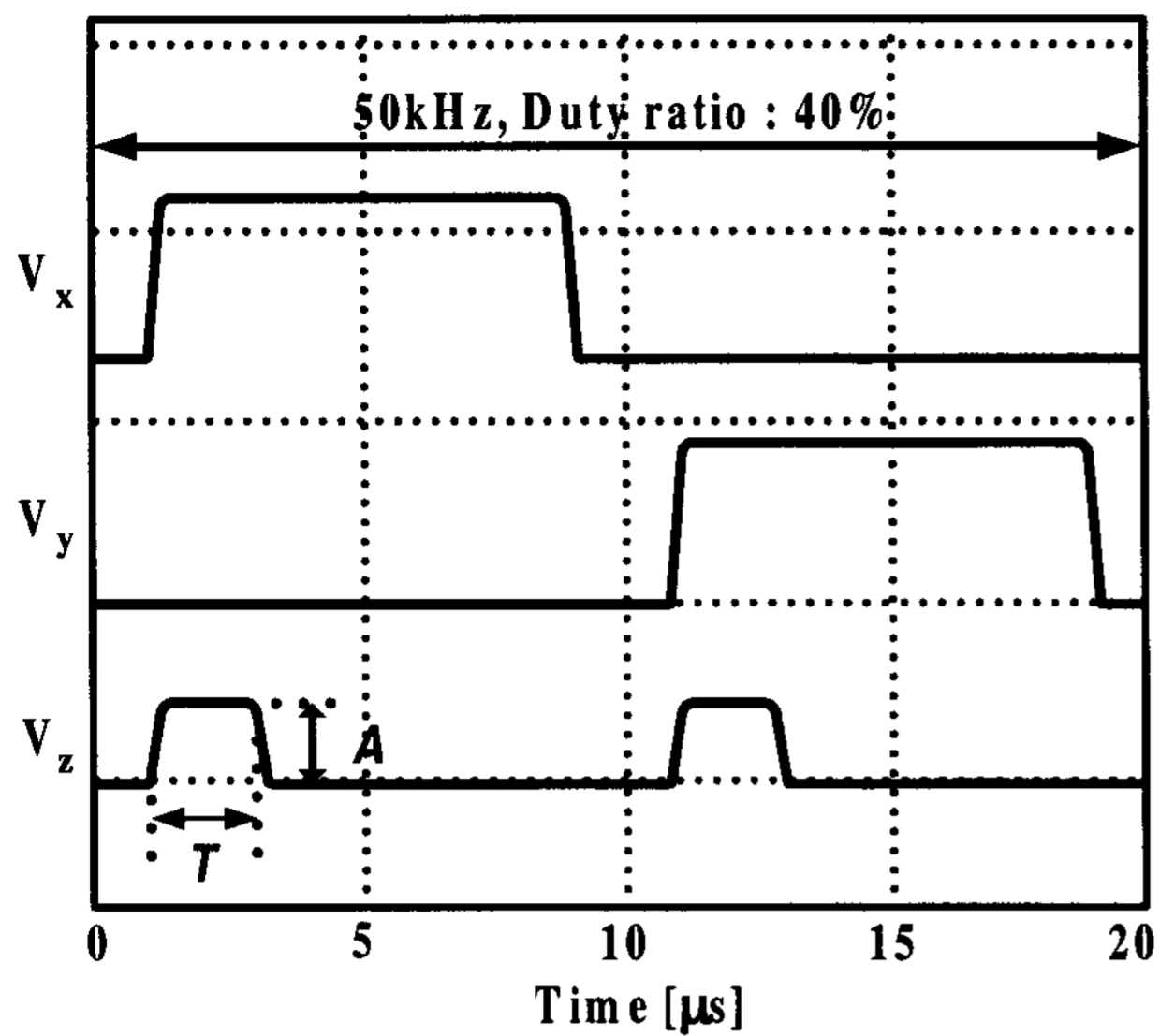
Fig. 1 shows the cell structure for positive column AC-PDP. Fig. 2(a) shows the pulse waveforms applied to three electrodes X, Y, and Z. The waveforms seem to be similar to the previous work [4] which used an auxiliary pulse on the address electrode Z in the conventional short gap discharge. However, in the longer gap (440 μm) discharge, the mechanism for producing a positive column discharge using those waveforms is entirely different. The pressure of 500 Torr and the mixture of Ne-Xe (4 %)-He are filled in this panel. Green phosphor ((Zn,Mn)₂SiO₄) is deposited between the barrier ribs. As shown in Fig. 2(a), the sustain voltage pulses with a duty ratio of 40 % are applied at a frequency of 50 kHz. The width T and the amplitude A of the pulse on the address electrodes are controlled from 0.6 μs and 0 V to 8 μs and 240 V, respectively. Even though V_z represents the whole waveform on the address electrode, the amplitude A is replaced with V_z in the figure and the discussion for the convenience of expression. The conventional electrode structure (electrode width: 390 μm , gap: 60 μm) as a reference is built in the same panel with long gap structure.

3. Results and Discussion

Fig. 2(b), (c), (d) shows the voltage distribution among the three electrodes as a parameter of time with respect to the waveform in Fig. 2(a) especially, when $V_z=0\text{V}$ (b), V_x or $V_y > 2V_z$ (c), and V_x or $V_y \leq 2V_z$ (d). The V_{xy} , V_{yz} and V_{zx} represent the V_x-V_y , V_y-V_z and V_z-V_x , respectively.

3.1 Firing Voltage

Fig. 3 shows the variation in firing voltage with the width T and amplitude V_z of the address short pulse. "Conv." indicates the



(a)

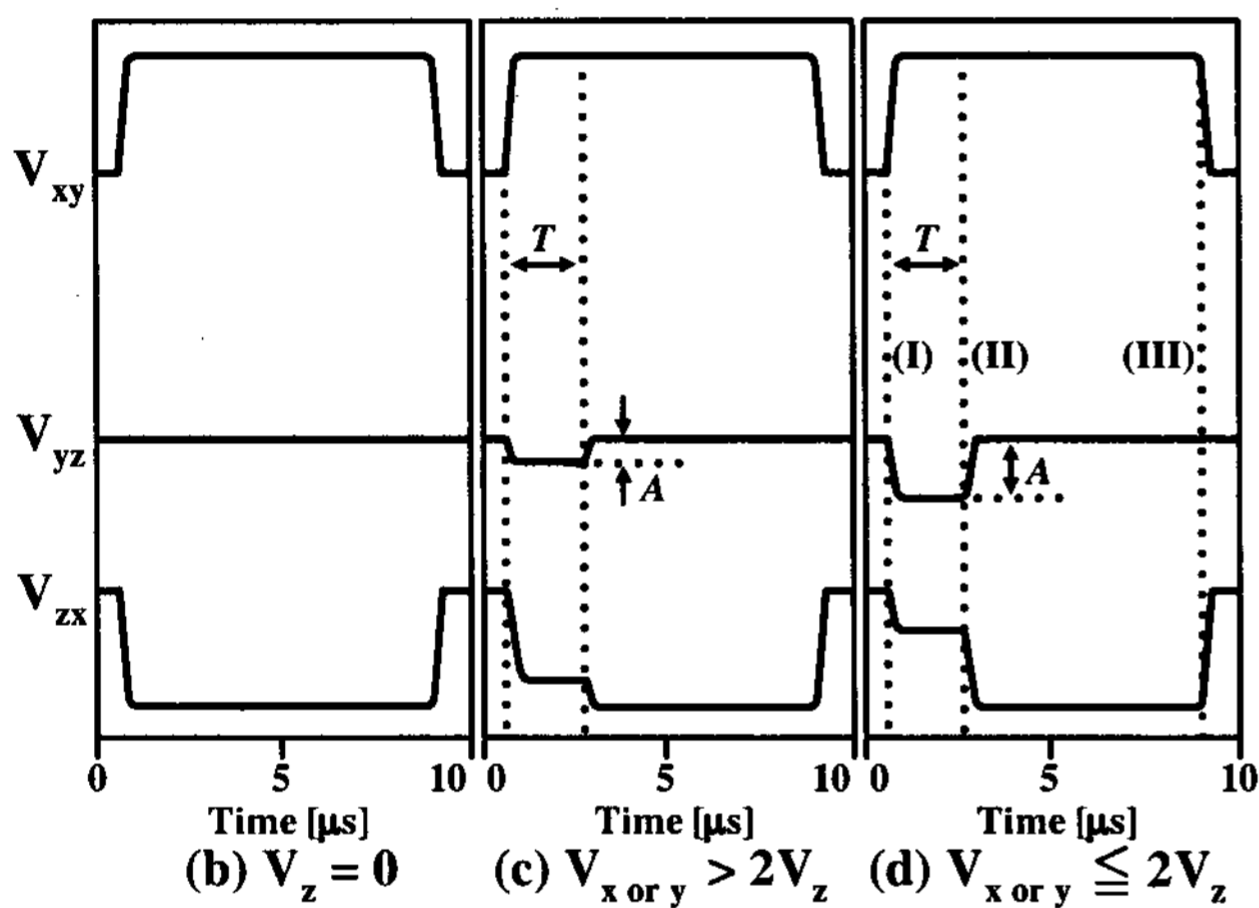


Fig. 2. Applied waveforms for positive column discharge(a) and voltage difference among three electrodes with time(b), (c), (d).

firing voltage of the conventional short gap (60 μm) case. When V_z increases, the firing voltage decreases abruptly except that the width T is 8 μs. The discharge is produced at around 400 V in V_z with 0 V, whereas the discharge is produced at about 200 V in V_z with 175 V. As shown in Fig. 4, when V_z is zero, the discharge starts up between the sustain and address electrodes X and Z by V_{zx} , then diffusing throughout the cell in a way that the ions are charged along the dielectric layer which covers the address electrode (i: ignition & diffusion). As the plasma approaches the electrode Y during the diffusion process, the effect of V_{xy} on maintaining the discharge between X and Y is intensified. Finally, the main discharge is generated between X and Y by V_{xy} (ii: main discharge). The direction of discharge process is denoted as the black arrow and the simple direction of electric field by the voltage difference is demonstrated by the white arrow in Fig. 4. In this case, the sustain electrode X works as an anode, meaning that the electrons are attracted to the electrode X. Even though the sustain dielectric is coated with high secondary emission material such as MgO, the secondary emission by the bombardment of

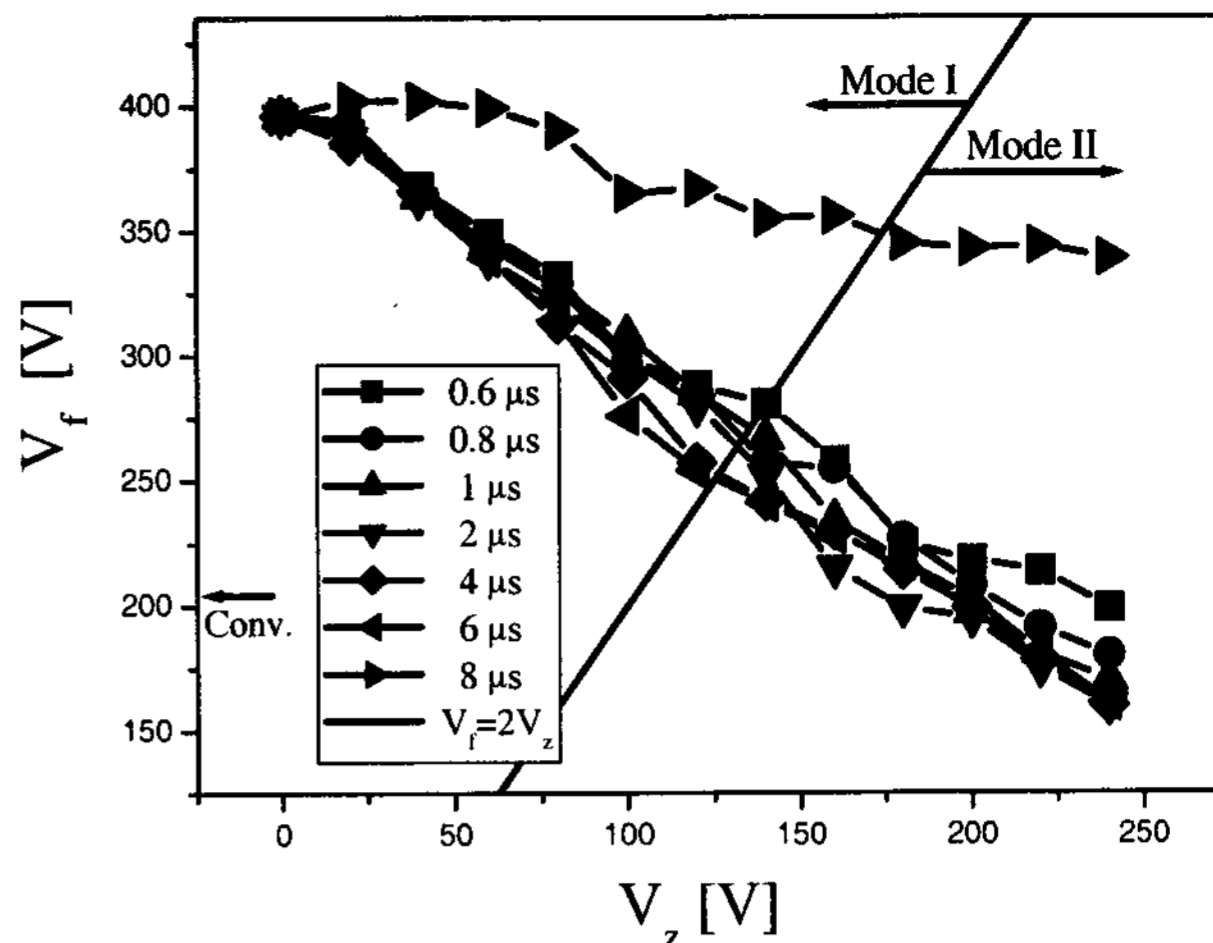


Fig. 3. Variation in firing voltage V_f with T and V_z .

electron is lower than that of ion. As such, the main discharge is initiated by means of general diffusion process. Thus, the firing voltage, when V_z is zero, is relatively high. As V_z increase, the mechanism of lowering the firing voltage can be explained in two modes which are classified by the generating direction of a long gap discharge process. For example, $V_f > 2V_z$ means $|V_{yz}| < |V_{zx}|$. Thus the triggering discharge ignites between the electrodes X and Z at the initial sustaining pulse. On the other hand, $V_f < 2V_z$ means $|V_{yz}| > |V_{zx}|$. Then the triggering discharge ignites between the electrodes Y and Z. When $V_f = V_z$, $|V_{yz}|$ is equal to $|V_{zx}|$. In this case, the discharge begins between the electrodes Y and Z since the ions with a higher secondary emission coefficient than that of the electrons bombard an MgO layer below the electrode Y. Therefore, the mode of discharge can be simply divided in two even though it is difficult to distinguish the discharge direction when V_f is slightly over $2V_z$. Mode I is when $V_f > 2V_z$ and Mode II is when $V_f \leq 2V_z$.

3.1.1 Firing Process of Mode I ($V_f > 2V_z$)

Fig. 5(a) shows the discharge mechanism of Mode I when $V_f > 2V_z$, as mentioned in Fig. 4. In Mode I, the ignition discharge is produced between the electrodes X and Z due to the electric field induced by V_{xy} and V_{zx} , then diffusing throughout the cell (i: ignition & diffusion). As V_z increases, V_{zx} decreases. However, since the distance between X and Z is shorter than that between X and Y, the ignition process itself does not need a high voltage. At some point during diffusion process, the discharge is attracted to the sustain electrode Y due to the help of the electric field induced by V_{yz} and V_{xy} . Finally, the main long gap discharge is established between the sustain electrodes X and Y by V_{xy} (ii: main discharge). Accordingly, the increase in V_{zy} by V_z allows the decrease of the firing voltage.

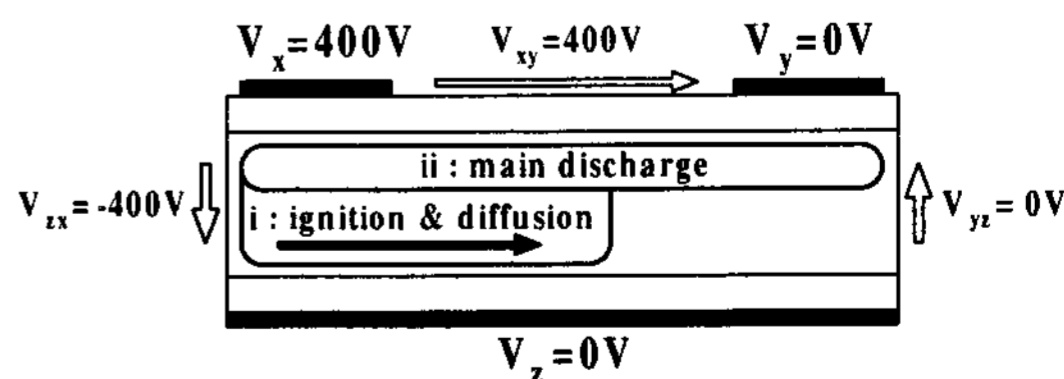


Fig. 4. Schematic of firing long gap discharge when $V_z=0V$.

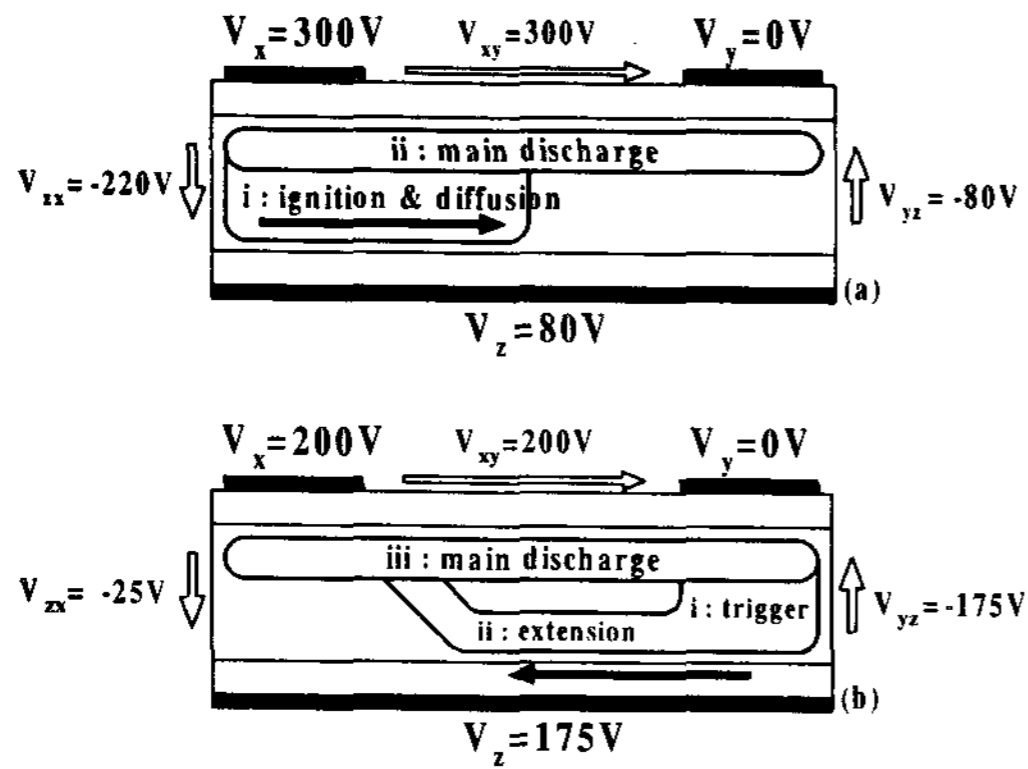


Fig. 5. Schematic diagram of firing positive column discharge at Mode I ($V_f > 2V_z$) (a) and Mode II ($V_f \leq 2V_z$) (b).

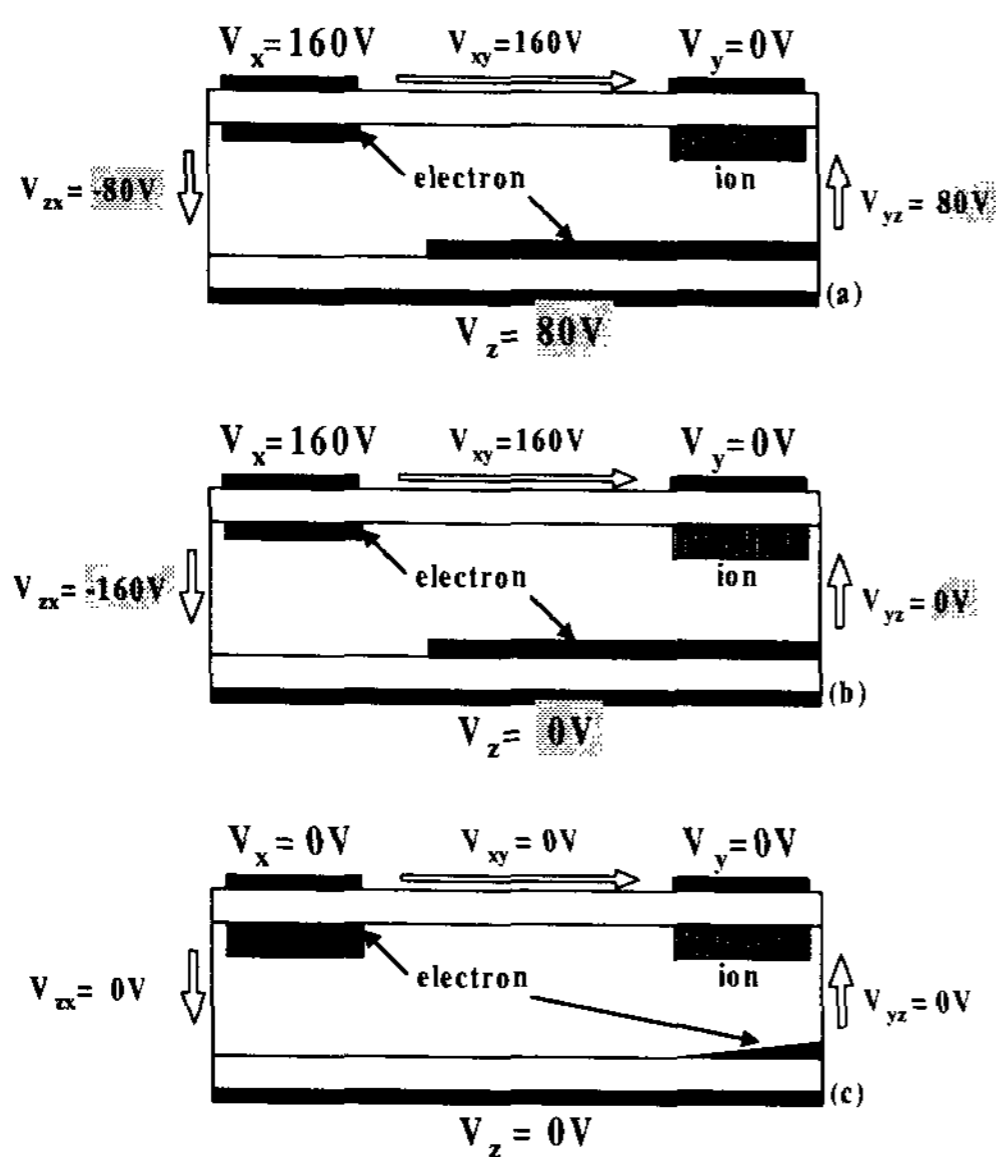


Fig. 6. Wall charge accumulation process for the consecutive positive column discharge between time step II and III. (a) just before time step II. (b) just after time step II. (c) after time step III.

3.1.2 Firing Process of Mode II ($V_f \leq 2V_z$)

Fig. 5(b) shows the discharge mechanism of Mode II. The discharge is triggered between Y and Z due to the electric field induced by V_{xy} and V_{yz} (i: trigger), then extending along the address electrode (ii: extension) by charging the electrons on the dielectric and phosphor layers. Finally, the discharge is connected to the electrode X (iii: main discharge). In addition, the electric field induced by V_{xy} and V_{zx} helps to construct the main discharge by attracting the extending discharge to the electrode X, which is coming through the electrode Z. The sustain electrode Y works as a cathode, so that the ions are attracted to the MgO layer covering the dielectric under the electrode Y. Thus, since the gamma coefficient of MgO is very high, the bombardment of ions enables the main discharge to be produced between X and Y at a lower firing voltage than that of Mode I. Since the trigger is generated by the electric field due to V_{xy} and V_{yz} , the increase of V_z contributes

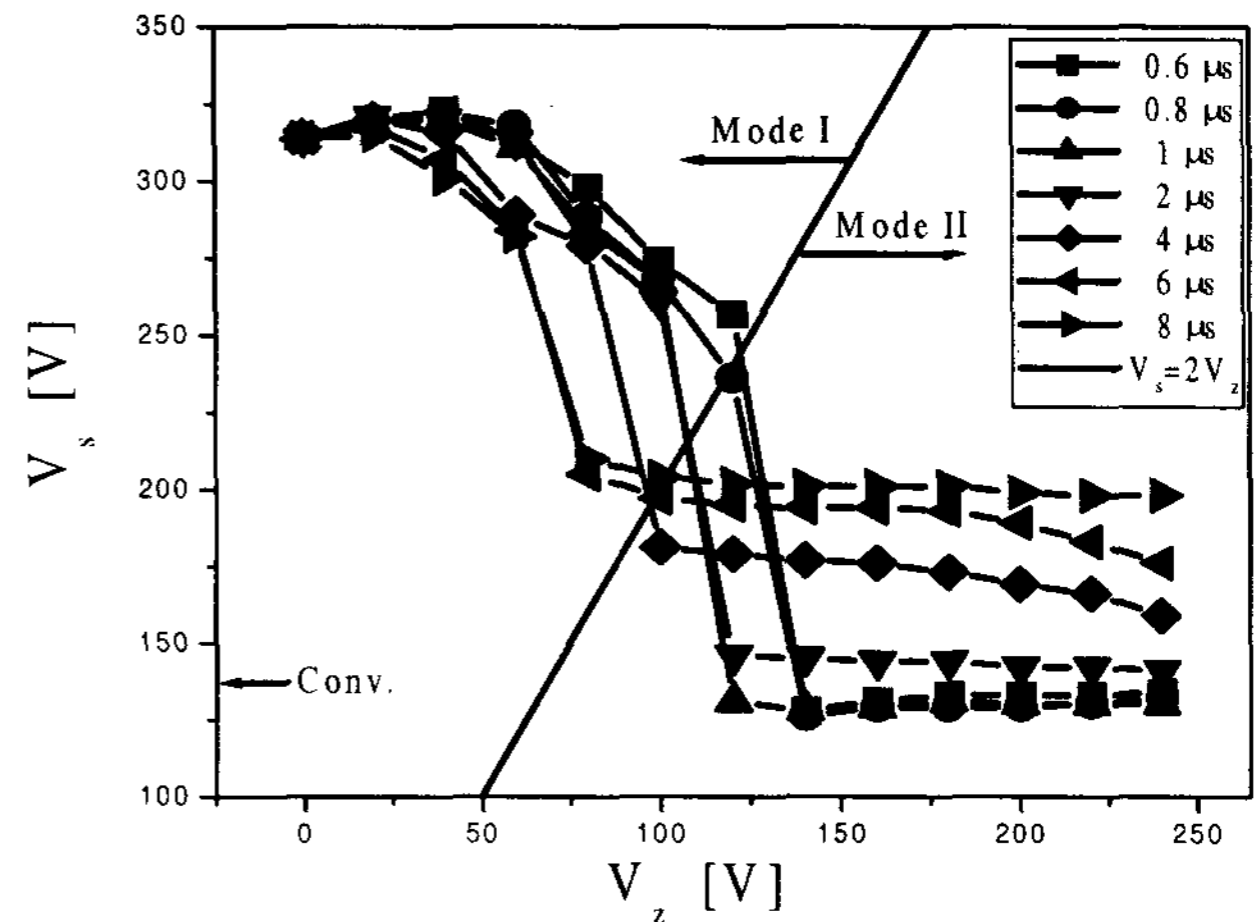


Fig. 7. Variation of sustaining voltage with T and V_z .

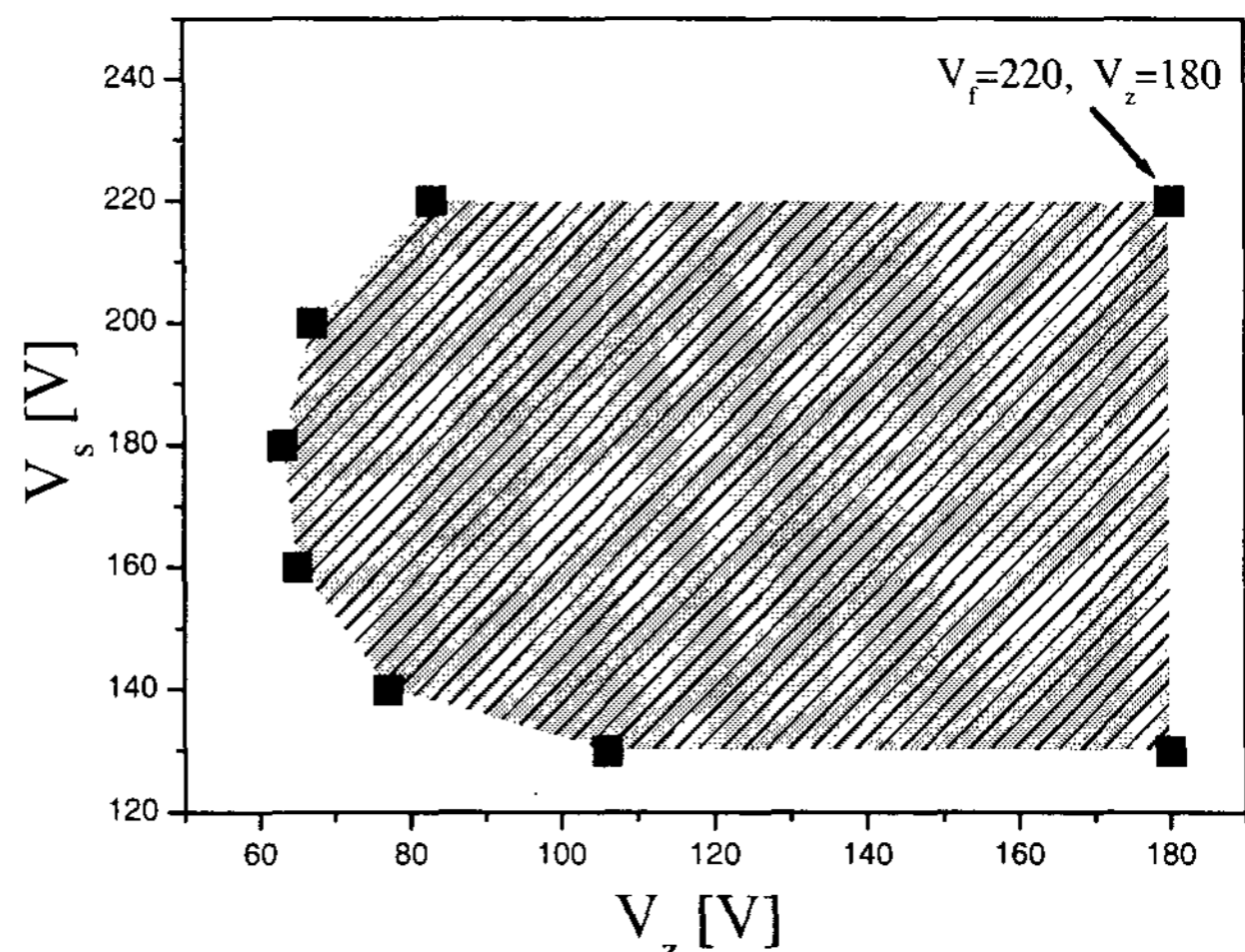


Fig. 8. Operational region in Mode II when $T = 0.6 \mu s$.

to the decrease of V_f . These processes occur between (I) and (II) in Fig. 2(d). In the case of T with $8 \mu s$, the firing voltage is still higher level than the others, even though V_z increases. As shown in Fig. 2(d), $T=8\mu s$ means that the level of V_{yz} and V_{zx} between II and III is the same level as that between I and II. This period is not directly connected to the firing process. In AC discharge, if the discharge is not sustained, the firing of the discharge can not be seen. Thus, it is reasonable that the firing voltage in $T=8 \mu s$ is analyzed from the view point of wall charge accumulation.

3.2 Sustaining Voltage

In Mode II, the discharge is extended by charging the electrons on the dielectric and phosphors covering the address electrode. This means that the electrons are accumulated between the periods I and II on there, however these charges are opposite to the consecutive triggering discharge and discharge extending procedure. Between the periods II and III in Fig. 2(d), V_{zx} erases these charges and converts space charges into wall charges on the electrode X, as shown in Fig. 6. As the time step II approaches the main discharge, the ions would be accumulated on the electrode Z and more electrons on the electrode X since there are more space

charges immediately after the discharge. $T = 8 \mu\text{s}$ means that there is no more erase or accumulation of wall charges between two electrodes X and Z between the periods II and III after the main discharge. Thus at $T = 8 \mu\text{s}$, the firing voltage does not change much due to the wall charge accumulation process between II and III. The effect of T is shown up more clearly in Fig. 7, which shows the sustain voltage characteristic with V_z and T . In Mode II, when the width T is getting longer, the sustain voltage is getting higher due to the wall charge accumulation process in Fig. 6. Also, Fig. 7 shows the boundary of Mode I and Mode II more clearly. The sustaining voltage decreases abruptly around the boundary $V_s = 2V_z$, implying that the discharge is unstable near the boundary.

3.3 Operational Voltage Range

Fig. 8 shows the operational region especially, when the discharge is fired at the firing voltage of 220V with 180V of V_z in the case of $T=0.6 \mu\text{s}$. It is clear that V_s and V_z can be controlled at very low level even at which the discharge is not sustained in Fig. 7. For example, the discharge is sustained stably when $V_s = 160 \text{ V}$ and $V_z = 80 \text{ V}$ in Fig. 8 however it is not in Fig. 7. This phenomenon is due to the independent control of V_s and V_z , namely, after the discharge is fired stably in Mode II region as $V_f=220\text{V}$, $V_z=180\text{V}$, V_z does not need to be 180V during the sustaining process. In other words, V_z only need to be kept the level which can trigger the main discharge. Therefore, the long gap discharge is established in extremely low sustaining voltage with considerably low voltage on the address electrode, as well as wide operational region.

3.4 Luminous Efficiency & Color coordinates

Fig. 9 shows the variation in the luminous efficiency with the T and V_z in Mode II at the sustaining voltage of 160 V. When V_z increases, the luminous efficiency decreases. The amplitude V_z is directly related to the intensity of triggering discharge since V_{zx} for triggering discharge varies with V_z . High voltage of V_z comes with strong triggering discharge which has low luminous efficiency. Most portions of the triggering discharge between the electrodes X and Z is in the negative glow region where the luminous efficiency is low since allowed discharge path between

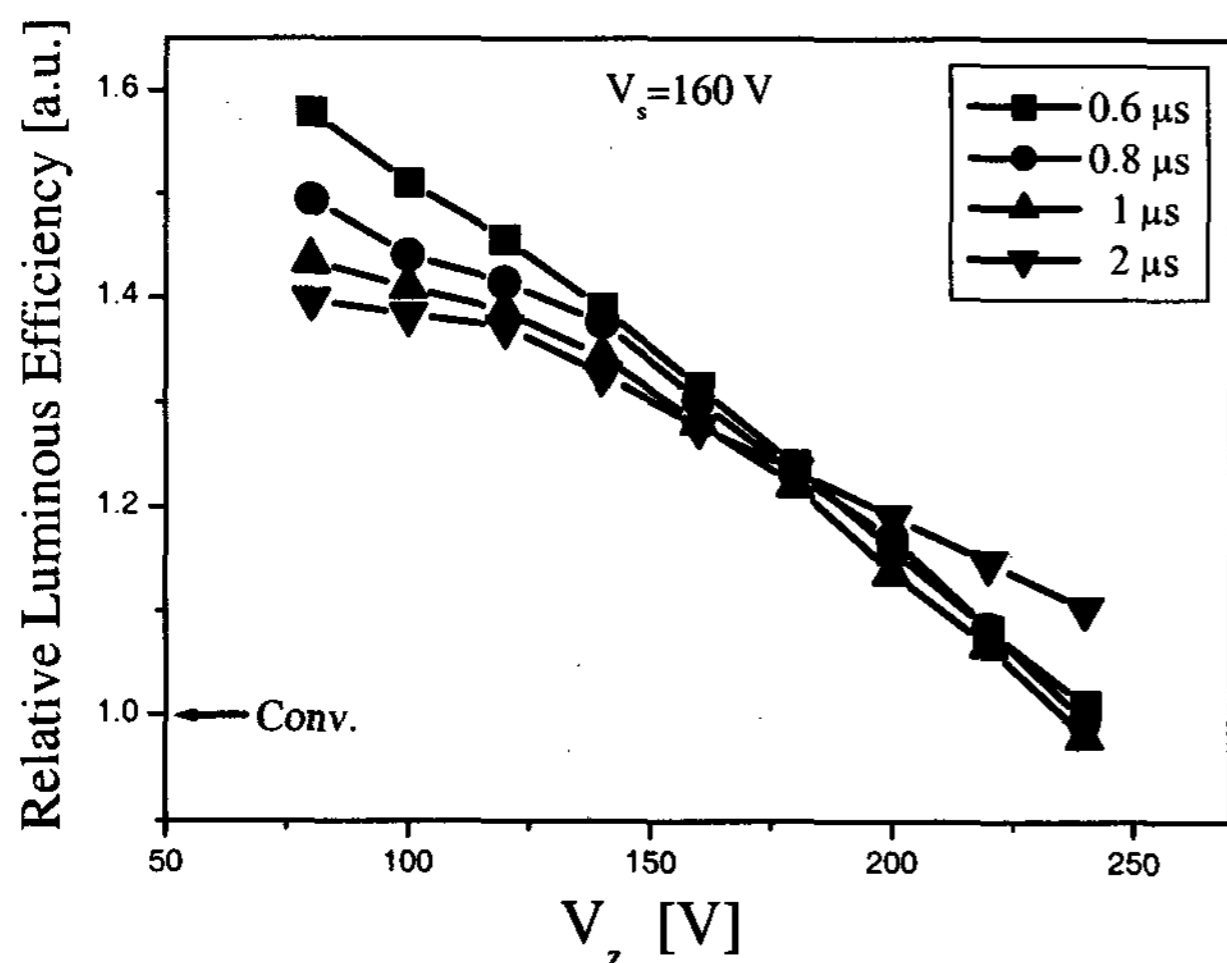


Fig. 9. Variations in relative luminance efficiency as a parameter of T and V_z in Mode II.

Table 1. Changes in CIE color coordinates of a green light

| V_z [V] | x | y |
|--------------|-------|-------|
| 80 | 0.248 | 0.705 |
| 100 | 0.248 | 0.704 |
| 120 | 0.248 | 0.704 |
| 140 | 0.249 | 0.704 |
| 160 | 0.250 | 0.703 |
| 180 | 0.251 | 0.702 |
| 200 | 0.252 | 0.702 |
| 220 | 0.253 | 0.701 |
| 240 | 0.255 | 0.699 |
| Conventional | 0.262 | 0.691 |

the sustain and address electrode is below $125 \mu\text{m}$. Consequently, the higher luminous efficiency comes from keeping the triggering discharge as small as it can trigger the main positive column discharge. The luminous efficiency increases by about 60% maximally in comparison with the conventional short gap discharge. Table 1 shows the changes in CIE color coordinates of green light. When V_z decreases, the color coordinate x decreases, whereas the y increases. This means the color purity of the green light is improved when the triggering discharge is controlled as small as it can triggers the main positive column discharge. Also, the variation of the color coordinate shows the existence of positive column, since the color coordinates between the negative glow and the positive column are different.

4. Conclusion

In this paper, long gap discharge characteristics are examined based on the control of voltage distribution among three electrodes for the positive column AC-PDP. By proper adjusting of the voltage difference among the three electrodes, the pulse width T on the address electrode is controlled for lower firing/ sustaining voltage and the intensity of triggering discharge is controlled for the better luminous efficiency of the positive column AC PDP. As a result, under the stable voltage margin condition, the firing and sustain voltages extremely decrease ($V_f=220\text{V}$, $V_s=150\text{V}$) and the color purity is improved, and finally, the improved luminous efficiency of about 60% is obtained in comparison with the conventional short gap case.

5. References

- [1] Larry F. Weber, United States Patent 6184848B1, 2001.
- [2] Jiting Ouyang, Thierry Callegari, Nicolas Lebarq, Bruno Caillier, and Jean-Pierre Boeuf, "Plasma Display Panel Cell Optimization : Modeling and Macro-cell Experiments", *Eurodisplay'02 Digest*, pp.53-56, 2002.
- [3] Thierry Callegari, Jiting Ouyang, Nicolas Lebarq, Bruno Caillier, and Jean-Pierre Boeuf, "3D modeling of a Plasma Display Panel Cell", *Eurodisplay'02 Digest*, pp.735-738, 2002.
- [4] Sang-Hun Jang, Ki-Duck Cho, Heung-Sik Tae, "Improvement of Luminance and Luminous Efficiency Using Address Voltage Pulse During Sustain-Period of AC-PDP", *IEEE Trans. Electron Devices*, vol. 48, pp. 1903-1910, September 2001.